Available online at www.sciencedirect.com
SCIENCE DIRECT®
Physics and Chemistry of the Earth 29 (2004) 579–587
PHYSICS and CHEMISTRY of the EARTH
www.elsevier.com/locate/pce

Change of ionospheric plasma parameters under the influence of electric field which has lithospheric origin and due to radon emanation

Y. Rapoport [a,*], V. Grimalsky [b], M. Hayakawa [c], V. Ivchenko [a], D. Juarez-R [d], S. Koshevaya [d], O. Gotynyan [a]

[a] Physics Faculty, Taras Shevchenko Kyiv National University, Prosp. Glushkov 6, 22 Kyiv, Ukraine
[b] National Institute for Astrophysics, Optics and Electronics, Z.P. 72000, Puebla, Pue, Mexico
[c] The University of Electro-Communications, 1-5-1 Chofugaoka, Chofu, 182-8585, Tokyo, Japan
[d] CIICAp, Faculty of Chemistry, Autonomous University of Morelos (UAEM), Av. Universidad, 1001, Z.P. 62210, Cuernavaca, Mor., Mexico

Received 30 May 2003; received in revised form 6 September 2003; accepted 22 September 2003
Available online 2 April 2004

Abstract

A mechanism of electric-photochemistry channel of seismo-ionospheric coupling is investigated. In particular, the penetration of electric field from the lithospheric source into the ionosphere and effect of this field on the photochemistry coefficient and ionospheric parameters in the altitude range in the lower D region are modeled numerically. It is shown that observable effects can be expected when lithospheric electric source strength is of the order of 1.5 kV/m. In this case, variations of electron temperature and electron concentration will be of the order of (40–60)% and (25–40)% respectively at the range of altitudes 60–70 km. An increase of near-ground conductivity (caused by increasing humidity and/or radon emanation) by ~2.3 times can cause increase of electric field intensity by ~2 times in altitude ranges of 60–70 km. Corresponding relative change of T_e increases up to ~50%, as compared with the case of lower near-ground temperature. Spatial shapes of relative distribution of electron temperature and the ratio of negative ion–electron concentration map the spatial shape of the lithospheric electric field distribution. Spatial shapes of electron concentration distribution and electric field strength distribution of the lithospheric source are "opposite" to each other.

1. Introduction

On the basis of observations of different seismo-ionospheric coupling phenomena, it is possible to reveal three main channels of seismo-ionospheric coupling before earthquakes. (1) Electromagnetic channel is connected with the penetration of electromagnetic signals radiated by lithospheric current source into the ionosphere (Molchanov et al., 1995; Grimalsky et al., 1999). Lithospheric currents can occur due to microfracturing which causes stochastic microcurrent activity (Molchanov and Hayakawa, 1994; Molchanov et al., 1995). Corresponding electromagnetic signals including ELF and VLF have been observed in the ionosphere before earthquakes (Molchanov et al., 1995). (2) Acoustic-gravity wave (AGW) channel (Gokhberg et al., 1996; Molchanov et al., 2001; Gotynyan et al., 2001) is characterized by radiation of AGW caused by greenhouse lithospheric gases. A lot of observed phenomena such as periodical variations in electron concentration in F ionospheric region (Gokhberg et al., 1996), variations of ionospheric glows (Gladishev and Fishkova, 1994), plasma turbulence in the F layer (Ossakov, 1981; Molchanov et al., 2002) etc. can be caused by AGWs generated before earthquakes. (3) Heating-photochemistry (Tomko et al., 1980; Fuks et al., 1997; Grimalsky et al., 2003; Dzubenko et al., 2003) and in particular electrostatic-photochemistry mechanism of seismo-ionospheric coupling is based on the following chain of processes: (a) increase of electron temperature due to electric field penetrating into the ionosphere from the lithosphere; (b) increase of electron collision frequency; (c) change of rate of energy exchange between charged particles and variations in the photochemistry coefficients, dynamics

* Corresponding author. Tel.: +380-44-266-4457; fax: +380-44-266-4507.
E-mail address: laser@i.kiev.ua (Y. Rapoport).

1474-7065/$ - see front matter © 2004 Elsevier Ltd. All rights reserved.
doi:10.1016/j.pce.2003.09.018

and steady-state conditions; (d) variations in the electron concentration and ionospheric conductivity (Fuks et al., 1997; Grimalsky et al., 2003), and one of possible consequences is the change in phase and losses of electromagnetic waves propagating in the "Earth-Ionosphere" waveguide (Molchanov and Hayakawa, 1998; Grimalsky et al., 2003; Dzubenko et al., 2003). The other possible mechanism which can cause variations in the temperature and ionospheric electron concentration (due to change of the heat conductivity and eddy diffusion coefficients) is AGW turbulence in the lower thermosphere (Didebulidze et al., 1990; Dzubenko et al., 2001, 2003).

Electrostatic-photochemistry mechanism is under consideration in the present work. Electrostatic mechanism of ionospheric heating is based on the following experimental facts. (1) Normal electric field of the order of 1 kV/m was observed in the lithosphere before an earthquake (Vershinin et al., 1999); (2) Radon concentration increased before and after earthquakes up to an order of value (Hayakawa et al., 1996; Huixin and Zuhuang, 1986); (3) In the presence of radon emanation, air conductivity is approximately proportional to radiation (Oster, 1965). In the presence of electric field excited by a strong source of lithospheric origin and of radon emanation before an earthquakes, electric field can penetrate up to the ionospheric altitudes and modify photochemistry processes through electron heating which influences photochemistry coefficients (see more details in Section 3 below).

In this paper, we consider the penetration of electrostatic field from the lithosphere into the ionosphere and its influence on photochemical and ionospheric parameters in the range of altitudes of the lower ionosphere. In particular, the following questions not considered before are studied. (1) In contrast to the papers by Tomko et al. (1980) and Fuks et al. (1997), electric field is not taken as a given value, but photochemistry steady-state conditions are investigated on the basis of solution of corresponding electrostatic 3D problem. (2) Influence of a variety of possible (experimentally observed) photochemistry parameters is under investigation in the present work, in distinction to previous papers on seismo-ionospheric coupling (see for example, Fuks et al., 1997). (3) Only modeling of photochemistry effect at a fixed altitude 60 km due to electric field penetrating from the lithospheric source has been done in Grimalsky et al. (2003). In the present article, an influence on photochemistry processes of the lithospheric electric field is calculated in the range of lower D region altitudes. (4) An influence of lithospheric electric field source spatial distribution shape on the electric-photochemistry effects in the lower D region before earthquakes is considered, in contrast to previous papers on electrostatic-photochemistry channel of seismo-ionospheric coupling.

2. Electrostatic-photochemistry model

Electrostatic-photochemistry model of seismo-ionospheric coupling includes two parts. At first, we have modeled penetration of electric field of lithospheric origin into the ionosphere. Then modification of ionospheric photochemistry processes due to the presence of electric field of the lithospheric origin before earthquakes is considered and possible changes of (measurable) ionospheric-photochemistry parameters are searched.

2.1. Electrostatic model

Electrostatic problem solved in the present paper is illustrated in Fig. 1. The aim of this calculation is to find electric field of the lithospheric origin penetrating into the ionosphere which will be used in the further calculations of the photochemistry parameters (in the parts (c) and (d) of the present section). The method of solution of electrostatic 3D problem was described in details in Grimalsky et al. (2003) and is only briefly repeated here. Three regions are included into the ionosphere model: I—region of isotropic media (atmosphere); II—region with finite conductivity where electrostatic field is of interest and is calculated; III—region with very large but finite longitudinal (relatively to geomagnetic field direction) conductivity where the "upper boundary condition" for the electrostatic potential, φ is used, namely $\varphi(z = Z_3) = 0$ (alternatively an "effective upper boundary condition" can be used, where the corresponding discussion can be found in Grimalsky et al. (2003)). Source dimensions $l_{X,Y}$ are of the order of 100 km, and fictitious lateral "walls" (Fig. 1) are used with distances between them $L_{X,Y} \gg l_{X,Y}$ (in particular values $L_{X,Y} \sim 1000$ km are chosen). Periodical boundary conditions at lateral "walls" and Fourier transform in the horizontal directions are used (see more details in Grimalsky et al. (2003)). Electrostatic problem $\mathrm{div}(\hat{\sigma}\nabla\varphi) = 0$, $\vec{E} = -\nabla\varphi$ is solved, where $\hat{\sigma}$ and $\vec{E}$ are conductivity tensor and electric field, respectively. Components of conductivity tensor in the system of coordinate connected with the geomagnetic field are

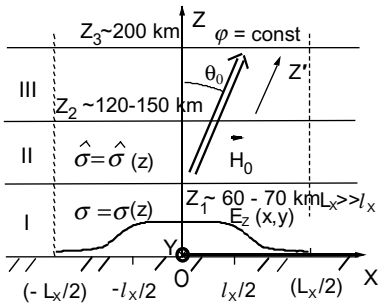

Fig. 1. Geometry of the electrostatic problem.

$$\sigma_3 = e^2 N_e \left(\frac{1}{m_e \nu_e} + \frac{1}{m_i \nu_i} \right),$$

$$\sigma_1 = e^2 N_e \left(\frac{\nu_e}{m_e(\omega_{He}^2 + \nu_e^2)} + \frac{\nu_i}{m(\omega_{Hi}^2 + \nu_i^2)} \right),$$

$$\sigma_H = e^2 N_e \left(\frac{\omega_{He}}{m_e(\omega_{He}^2 + \nu_e^2)} - \frac{\omega_{Hi}}{m_i(\omega_{Hi}^2 + \nu_i^2)} \right),$$

where N_e, $\nu_{e,i}$, $m_{e,i}$, $\omega_{pe,i}$, $\omega_{He,i}$ are electron concentration, electron and ion collision frequencies, masses, plasma frequencies and cyclotron frequencies, respectively; σ_3, σ_1 and σ_H are parallel, Pedersen and Hall conductivities respectively (Gurevich, 1978). In the lower D region ($z \sim 60$ km), ionosphere is isotropic, $\sigma_H \ll \sigma_p = \sigma_\parallel \approx \frac{e^2 N_e}{m\nu_e}$. Heating of electron gas is determined by following equations (Gurevich, 1978):

$$\frac{d\theta}{dt} = \frac{2}{3} Q - \delta(\theta)\nu_e(\theta)(\theta - 1). \tag{1a}$$

Here $Q = \mathrm{Re}(\sigma_{ij} E_i E_j)/(N_e T_e)$, σ_{ij} and $E_{i,j}$ are the components of conductivity tensor and of electric field respectively in the coordinate system with OZ axis directed vertically upward (see Fig. 1). The summation by repeated indexes is supposed. Components σ_{ij} are determined by components σ_3, σ_1 and σ_H and the angle θ_0 between the vertical direction and the direction of geomagnetic field (Fig. 1),

$$\nu_e(\theta) = \nu_{e0}\theta^{5/6}, \tag{1b}$$

$\theta = T_e/T_{e0}$ is relative electron temperature, T_{e0} is the unperturbed value of T_e, $\delta(\theta)$ is the rate of energy, transmitted from electrons to neutral particles under collisions. In the lower D region, $Q \approx \sigma_P E_z^2$ (taking into account that in our problem, the vertical component of the electric field in this region is much larger than the other components).

To characterize "how nonlinear" the influence of the penetrating field on the ionosphere is, and how effective electron gas heating can be, this field should be compared with the "characteristic ionospheric electric field" which is determined as follows (Gurevich, 1978):

$$E_p = \sqrt{3T_n \frac{m_e}{e^2} \delta(T_n)\nu_e(T_n)}, \tag{1c}$$

where e is electron charge, and $T_n = T_{e0}$. In the present paper, we are interested more in electron gas heating than in possible nonlinearity of the ionosphere heated by electrostatic field of lithospheric origin (the last problem should be considered separately). In particular, we can expect that if the electrostatic field of lithospheric origin penetrating into the D region of the ionosphere is even a few times less than the value of E_p, an observable change in electron temperature is possible. When the value of electrostatic field of lithospheric origin is close to E_p, the corresponding electron heating should be very essential (Gurevich, 1978).

2.2. Photochemistry model

This model describes the set of (main) photochemistry reactions in the lower ionosphere (Rowe et al., 1974; Tomko et al., 1980; Martinenko, 1989; Tohmatsu and Ogawa, 1991). Examples of these reactions are presented below:

$O_2 + O_2 + e \rightarrow O_2^- + O_2$ (reaction of three-body electron attachment to O_2 with the participation of O_2 as the "third body");
$O_2 + N_2 + e \rightarrow O_2^- + N_2$ (reaction of three-body electron attachment to O_2 with the participation of N_2 as the "third body");
$O_2^- + O \rightarrow O_3 + e$ (reaction of collisional electron detachment from O_2^- under collision of O_2^- with atom O);
$O_2^- + O_2(^1\Delta g) \rightarrow 2O_2 + e$ (reaction of collisional electron detachment from O_2^- under collision of O_2^- with excited molecule $O_2(^1\Delta g)$);
$h\nu + O_2 \rightarrow O_2^+ + e$ (reaction of electron photodetachment);
$NO^+ + e \rightarrow N + O$ (reaction of dissociative recombination);
$O_2^+ + e \rightarrow O + O$ (reaction of dissociative recombination);
$O_2^+ + X^- \rightarrow O_2 + X$ (ion–ion recombination reaction).

Charge conservation law has the form: $N_{NO^+} + N_{O_2^+} + N_{Y^+} - N_{O_2^-} - N_{X^-} - N_e = 0$, where N_{X^-}, N_{Y^+} are concentrations of all other negative particles besides O_2^- (NO_3^-, CO_3^-, CO_4^- etc.), denoted as X^-, and positive (water) cluster groups $H^+ \bullet (H_2O)_n$, denoted as Y^+, respectively (model by Rowe et al. (1974)).

2.3. Effective photochemistry coefficients

In the approximation used, effective photochemistry coefficients (Tohmatsu and Ogawa, 1991; Martinenko, 1989; Fuks et al., 1997) are determined in accordance with the simplified model (Tohmatsu and Ogawa, 1991) where effective coefficients of electron attachment, β, electron detachment, γ, dissociative recombination, α_D and ion–ion recombination, α_i are determined as values averaged by corresponding concentrations, namely:

2.3.1. Coefficient of dissociative recombination

$$\alpha_D = (\alpha_{DNO^+}[NO^+] + \alpha_{DO_2^+}[O_2^+] + \alpha_{Y^+}[Y^+])/N^+,$$

where $N^+ = [NO^+] + [O_2^+] + [Y^+]$ is the total positive ion concentration, symbol [A] means concentration of particles of specific A, values α_{DNO^+}, $\alpha_{DO_2^+}$, α_{Y^+} are coefficients of dissociative recombination of corresponding ions.

2.3.2. Coefficient of electron detachment (γ)

$$\gamma = \frac{\gamma_{O_2^-}[O_2^-] + \gamma_{X^-}[X^-]}{[O_2^-] + [X^-]}, \tag{2}$$

where $\gamma_{O_2^-}$, γ_{X^-} are electron detachment coefficients for corresponding ions and

$$\gamma_{O_2^-} = \gamma_{ph} + K_1[O_2(^1\Delta_g)] + K_2[O(^3P)] + K_3[O_2] + K_4[N_2] + K_5[O],$$

where γ_{ph} is the electron photo-detachment coefficient; K_1, K_2, K_3, K_4 and K_5 are the coefficients of electron detachment from the ions O_2^- under the collisions of O_2^- with excited molecules $O_2(^1\Delta_g)$, atoms $O(^3P)$, molecules O_2, molecules N_2 and atoms O, respectively. These coefficients are presented in Tomko et al. (1980), Martinenko (1989) and Ogawa and Shimazaki (1975). It is important for the present problem to emphasize dependencies of photochemistry coefficients on electron temperature, T_e (Tomko et al., 1980; Martinenko, 1989) which is modified by electric field of lithospheric origin: for electron attachment coefficient,

$$\beta = 1.4 \times 10^{-29} \frac{300}{T_e}[O_2]^2 e^{-\frac{600}{T_e}} + 10^{-31}[O_2][N_2], \tag{3}$$

where T_e is in eV, concentrations $[O_2]$, $[N_2]$ are in cm^{-3}; for dissociative recombination coefficients

$$\alpha_{DNO^+} \sim (T_e/T_n)^{-0.5}; \quad \alpha_{DO_2^+} \sim (T_e/T_n)^{-0.6};$$

$$\alpha_{Y^+} \sim \left(\frac{T_e}{T_n}\right)^{-b}, \quad 0.2 \leqslant b \leqslant 1, \tag{4}$$

where T_n is neutral particle's temperature. In the lower ionospheric D region $T_n \approx T_{e0}$. The dependence of electron collision frequency, ν_e on T_e is described by relationship (1b).

2.4. Altitude distributions of the ion concentrations and photochemistry coefficients

It is relevant to show which photochemistry parameters are used in the present calculations because a wide scatter of experimental data presented in different publications is rather typical in particular for the lower ionosphere. Data used for some of the ion constituents (Ogawa and Shimazaki, 1975) are shown in Fig. 2(a). Emphasize that electron concentration reported in some other papers, are about one order of magnitude larger than in Ogawa and Shimazaki (1975). Corresponding photochemistry coefficients are calculated on the basis of data (Ogawa and Shimazaki, 1975) and formulas presented above (such as Eq. (1)). An example of such calculations for dissociative recombination coefficient is shown in Fig. 2(b). Altitude dependence of this coefficient reflects peculiarity of the positive ion distribution in the lower D region, namely decrease of water cluster concentration and increase of concentrations of other positive ions with altitude (Fig. 2).

In this paper, we consider steady-state conditions. In particular, steady-state electron concentration can be obtained from the simplified model (Tohmatsu and Ogawa, 1991) on the basis of a set of equations (Fuks et al., 1997; Tohmatsu and Ogawa, 1991):

$$\frac{dN^-}{dt} = \beta N_e - \gamma N^- - \alpha_i N^- N^+, \tag{5a}$$

$$\frac{dN^+}{dt} = q - \alpha_i N^- N^+ - \alpha_D N^+ N_e \tag{5b}$$

$$N_e = N^+ - N^-, \quad \lambda = N^-/N_e,$$

where q is electron production rate, α_i is ion–ion recombination coefficient. Putting $\frac{d}{dt} = 0$, one can get from Eqs. (5a) and (5b):

$$\beta - \gamma\lambda - \alpha_i\lambda(1+\lambda)\sqrt{\frac{q}{(\alpha_D + \lambda\alpha_i)(1+\lambda)}} = 0, \tag{6}$$

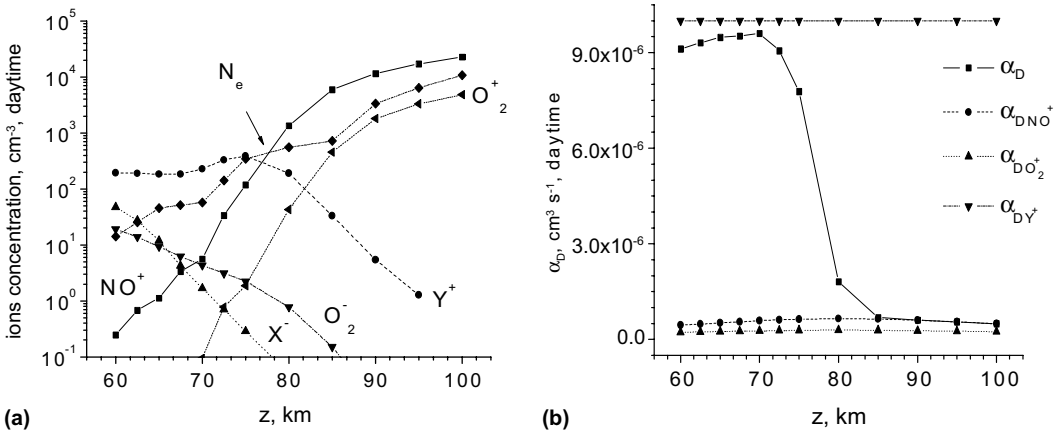

Fig. 2. Altitude dependence of ion concentrations (a) and dissociative recombination rates (b) for different ions in daytime (on the basis of data (Ogawa and Shimazaki, 1975)).

If $\gamma \gg \alpha_i N^+$ (which is satisfied in the lower D region), then Eq. (6) gives $\lambda = \beta/\gamma$, and it is possible to get the following from Eqs. (5a) and (5b) (Tohmatsu and Ogawa, 1991; Fuks et al., 1997):

$$N_e = \sqrt{\frac{q}{(\lambda\alpha_i + \alpha_D)(1+\lambda)}},$$
$$\frac{N'_e}{N_{e0}} = \sqrt{\frac{(\lambda_0\alpha_i + \alpha_{D0})(1+\lambda_0)}{(\lambda'\alpha_i + \alpha'_D)(1+\lambda')}}. \quad (7)$$

In Eq. (7), $\lambda_0 = \lambda(T_e = T_{e0})$, $\alpha_{D0} = \alpha_D(T_e = T_{e0})$ and $\lambda' = \lambda(T'_e)$, $\alpha'_D = \alpha_D(T'_e)$ $\alpha'_D = \alpha_D(T'_e)$ are unperturbed and perturbed values due to the presence of the electric field, respectively, N_{e0}, T_{e0} and N'_e, T'_e are unperturbed and perturbed values of electron concentration and temperature, respectively.

Effect of electron heating can be explained in a simplified manner as follows. If T_e increases, $\beta(T_e)$ increases as seen from Eq. (3), and N_e decreases in accordance with Eq. (7). This behavior of N_e in steady-state conditions corresponds qualitatively to the results obtained using the photochemistry dynamical model (Grimalsky et al., 2003; Tomko et al., 1980) in the steady-state limit.

3. Results of modeling

In Fig. 3, typical altitude distributions of conductivity tensor elements used in the present calculations are shown. Corresponding altitude dependence of electric field is shown in Fig. 4(a) and for higher near-ground conductivity in Fig. 4(b). This increase of conductivity may be caused by higher humidity and by radon emanation before an earthquake. Calculations have been done for a "single" lithospheric electric field source (i.e. source with spatial distribution having one maximum) in the form

$$E_Z(z=0,x,y) = E_0[1 + \xi/ch^2(x/l_X)ch^2(y/l_Y)], \quad (8)$$

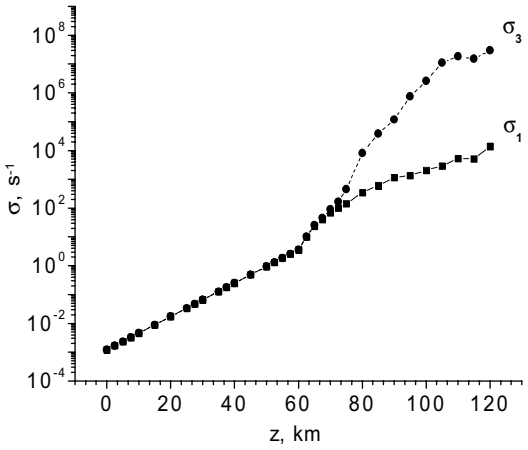

Fig. 3. Dependence $\sigma_{1,3}$ (elements of conductivity tensor) on altitude for daytime.

where E_0 (~100 V/m) is the fine weather electric field strength, ξ and $l_{X,Y}$ are the ratio of lithospheric electric field strength to fair weather field strength and characteristic source dimensions in X, Y directions respectively. The maximum electric field value taken for calculations is equal to $E_Z(z=0,x=0,y=0) = E_0(1+\xi) = 1.5$ kV/m. As seen from Fig. 4(b), an increase of near-ground conductivity by ~2.4 times leads to the corresponding increase of electric field which is, as a result, of the same order or even exceeds the ionospheric characteristic field, E_p at the corresponding altitudes. Therefore rather effective heating of electron gas can be expected, which is proven by calculations shown in Fig. 5.

As seen from Figs. 4 and 5, in the presence of lithospheric electric field with strength of the order of 1.5 kV/m, electron temperature can exceed the unperturbed value by 10–30% in altitude range 60–70 km and by 10–100% in a case of increasing near-ground conductivity. Fig. 6 shows altitude variations of dissociative recombination effective perturbed coefficient, electron collision

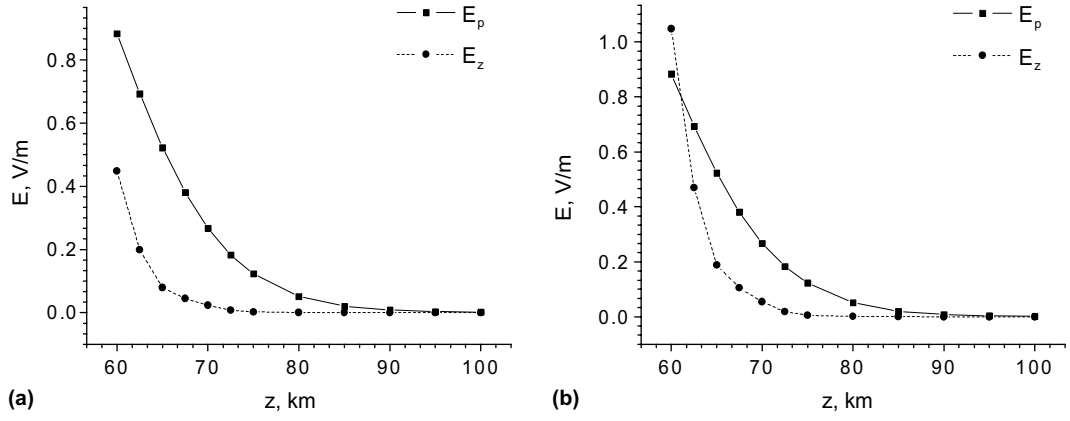

Fig. 4. Altitude distribution of vertical component of electric field (E_z) and characteristic electric field (E_p), (a) conductivity ratio σ(60 km)/σ(0 km) = 3×10^3, (b) higher near-ground conductivity, σ(60 km)/σ(0 km) = 1.2×10^3.

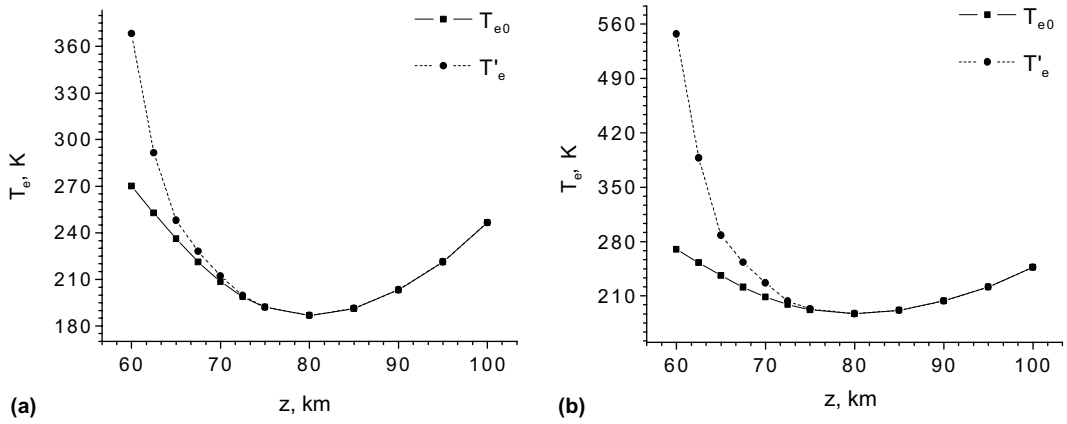

Fig. 5. Dependence of electron temperature on the vertical coordinate above the center of earthquake preparation region in the absence and in the presence of electric field (T_{e0}, T'_e, respectively), (a) conductivity ratio $\sigma(60\text{ km})/\sigma(0\text{ km}) = 3\times10^3$; (b) higher near-ground conductivity (see the conductivity ratio value in the caption of Fig. 5).

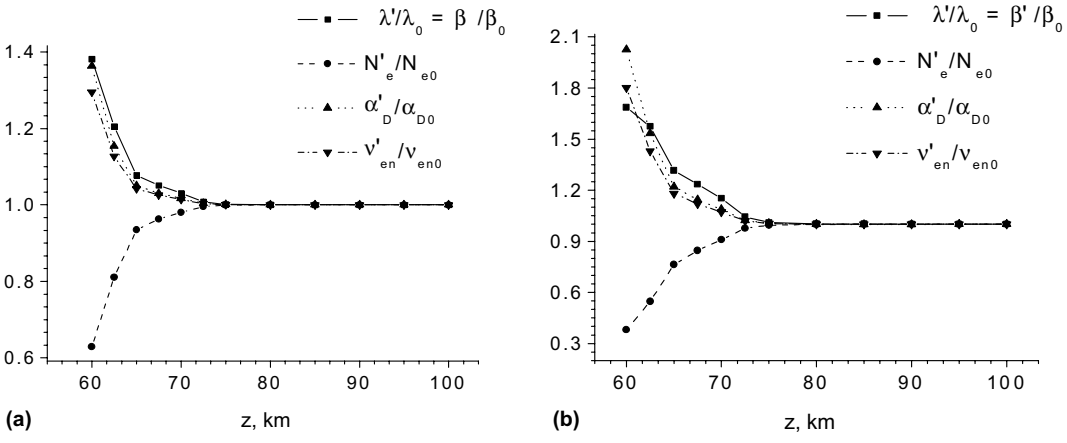

Fig. 6. Altitude distribution of normalized values of perturbed effective dissociative recombination coefficient (α'_D/α_{D0}), ratio of negative ions concentration to electron concentration (λ'/λ_0), electron collision frequency (ν'_{en}/ν_{en0}) and electron concentration (N'_e/N_{e0}) above the center of earthquake preparation region: (a) conductivity ratio $\sigma(60\text{ km})/\sigma(0\text{ km}) = 3\times10^3$; (b) higher near-ground conductivity, see the caption of Fig. 4.

frequency and electron concentration. It is seen that, as a result of heating, electron concentration decreases from 10% to ~40% in the range of altitudes 70–60 km, and the absolute value of relative change of electron concentration can increase up to ~70%, if near-ground conductivity increases (Fig. 6(b)). Relative change of electron conductivity can reach the value 30–80% in the altitude range 70–60 km. The effect of shape of lithospheric electric field spatial distribution, which has in particular two maxima in the horizontal plane, Fig. 7 (in distinction to distribution (8)) is illustrated in Figs. 8–10. It is seen that spatial shape of electron temperature distribution (Fig. 8) and negative ions–electron concentration ratio (Fig. 10) map the spatial shape of the lithospheric source electric field (Fig. 7). Spatial shapes of electron concentration distribution and electric field distribution of the lithospheric source (Figs. 9 and 7, respectively) are "opposite" to each other.

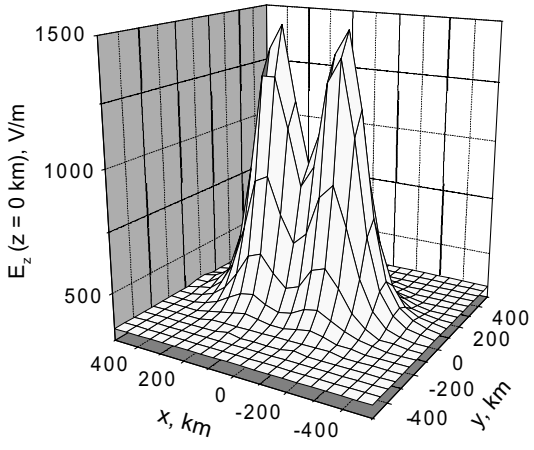

Fig. 7. Spatial distribution of electrostatic field from double lithospheric source at $z = 0$.

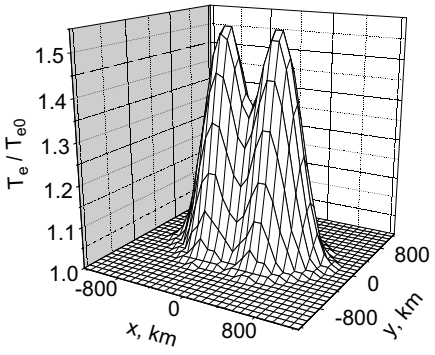

Fig. 8. Spatial distribution of normalized perturbed electron temperature for double source (Fig. 7), $z = 60$ km, nighttime, $\sigma(60\text{ km})/\sigma(0\text{ km}) = 3.6/1.2\times10^{-3} \approx 3\times10^{3}$.

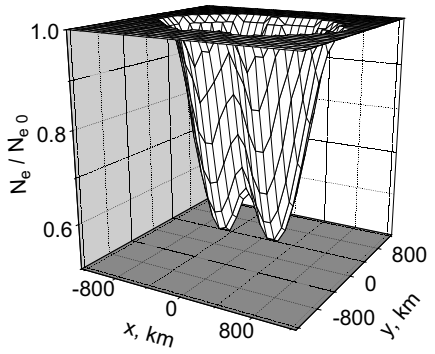

Fig. 9. Spatial distribution of normalized electron perturbed concentration for double source (Fig. 7), $z = 60$ km, nighttime.

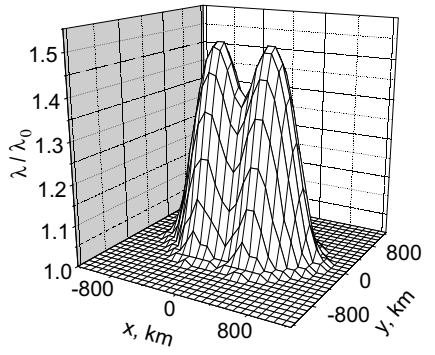

Fig. 10. Spatial distribution of normalized ratio of negative ions concentration to electron concentration, for double source (Fig. 7), $z = 60$ km, nighttime.

Fig. 11 shows that possible variation of photochemistry parameters (Tomko et al., 1980), namely increase of values of γ_{X^-}, b which characterize electron detachment from negative ions and dissociative recombination with (positive) water clusters respectively, leads to a moderate increase of relative change of electron concentration due to heating by the electric field.

Calculations have been done also for other dataset taken from Rowe et al. (1974). This dataset corresponds

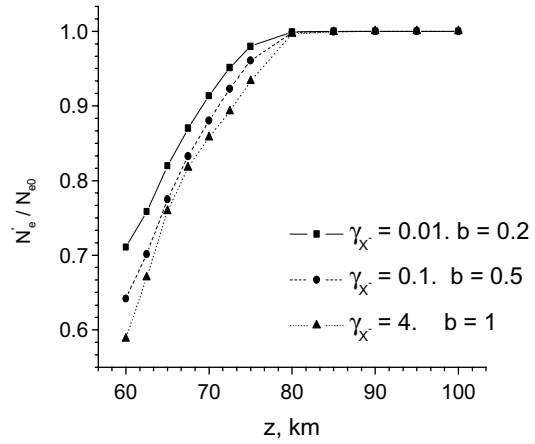

Fig. 11. Altitude dependence of normalized perturbed electron concentrations for different γ_{X^-} and b during daytime.

to higher (by about 5 times) values of electron concentration and higher concentrations of some of the ions comparatively to those used in the calculations presented above and taken from Ogawa and Shimazaki (1975). Corresponding values of relative change of electron concentration caused by electron gas heating by electric field are about 50% less than those shown in Fig. 6.

4. Discussion and conclusions

A possible observable effect caused by the electrostatic field before earthquakes in the altitude range 60–70 km is shown. Relative change of electron concentration and electron temperature of the order of a few dozens percent in this range of altitudes (namely, 20–50% at different altitudes and for different values of the lithospheric electric field strength) is possible. Rather strong electrostatic lithospheric source with field strength of the order of 1.5 kV/m is necessary for this. As a result of increasing near-ground conductivity caused by increased humidity and radon emanation, maximum relative change of electron temperature in this range of altitudes can reach a value of the order of 100%, corresponding relative change of electron concentration reaches a value of the order of 70%, and maximum relative change of electron conductivity reaches a value of the order of 60%. We have analyzed ionospheric response to electrostatic field excited by lithospheric sources of different spatial shapes. This question is important due to the following reason. Any channel of seismo-ionospheric coupling describes a definite set of energy transformations in a layered inhomogeneous system, lithosphere–atmosphere–ionosphere. To describe such a process adequately, it is necessary to solve a problem of excitation of corresponding disturbances by lithospheric source, their

penetration into and effect on the ionosphere and finally to try to find reflection of some of the characteristic features of seismic source in the ionospheric response. Recently, connection between spatial (shape) and temporal (frequency) characteristics of lithospheric source and ionospheric response have been investigated for electromagnetic (Grimalsky et al., 1999; Grimalsky et al., 2002) and AGW (Gotynyan et al., 2003) channels of seismo-ionospheric coupling. It is shown in the present paper that spatial shape of the ionospheric disturbances of electron temperature and concentration is similar to the shape of lithospheric electric field spatial distribution.

Change of electron concentration and conductivity can give some contribution to observable changes of parameters (phase and amplitude) of electromagnetic waves propagating in the waveguide "Earth-Ionosphere" before earthquakes (Hayakawa et al., 1996; Molchanov and Hayakawa, 1998). At the same time, present consideration shows that possible remarkable change of electron concentration and temperature is restricted by the altitudes of the lower D region, namely 60–70 km. It is worthwhile to consider a possibility of thermal instability (Gurevich, 1978) in the D region of the ionosphere in the presence of electrostatic field of the lithospheric origin. If such an instability is possible, effects considered in the present paper can increase by value and maybe change of electron concentration and conductivity can take place at altitudes higher than 60–70 km. Electric field with strength of the order of (0.5–10) V/m has been observed in the D region (Fuks et al., 1997). Such fields may be connected with some sort of heating instability, and penetration of seismogenic electrostatic field into the D region may possibly favor such an instability development. Such a problem is out of the scope of the present paper and may be a subject of our separate work.

Finally, the following conclusions can be summarized.

(1) At the different altitudes, the value of the electric field with lithospheric origin is a few times less than or of the same order as the corresponding ionospheric characteristic field, E_p (Fig. 4(b)). As a result, ionospheric electric field of lithospheric origin (with source strength $E_z(z=0) \sim 1.5$ kV/m) can significantly affect electron temperature (up to ~40–60%, Figs. 5 and 8) and concentration (up to 25–40%, Figs. 6 and 9) in the range of altitudes $Z \sim (60–70)$ km, where electric strength reaches a value $E \sim 0.2–1$ V/m (Fig. 4).
(2) An increase of near-ground conductivity (caused by increasing humidity and/or radon emanation) can cause an increase in electric field (compare Fig. 4(a) and (b)) and electron temperature at altitude 60–70 km. In particular, ~2.3 times increase of near-ground conductivity causes an increase of values of electric field by ~2 times (Fig. 4(a) and (b)) in the ranges of altitude 60–70 km. Corresponding relative change of T_e can increase up to more than ~50% as compared to the case of lower near-ground conductivity (Fig. 5(a) and (b)).
(3) Variation of initial parameters (from $\gamma_{X^-} = 0.01$, $b = 0.2$ to $\gamma_{X^-} = 4$, $b = 1$), which characterizes electron detachment from negative ions and dissociative recombination with (positive) water clusters (see Eqs. (2) and (4)), respectively, can lead to an increase of relative change of electron concentration of about 15–20% in the range of altitudes 70–60 km (Fig. 11).
(4) Spatial shapes of distribution of electron temperature (Fig. 8) and negative ion–electron concentration ratio (Fig. 10) repeat the spatial shape of the lithospheric electric source (Fig. 7). Spatial shapes of electron concentration distribution and electric field distribution of the lithospheric source (Figs. 7 and 9, respectively) are "opposite" to each other.
(5) Finally, we emphasize that not only radon near-ground concentration (or conductivity) increase is enough to cause remarkable increase of electric field and therefore change of photochemistry dynamics and steady-state conditions in the ionosphere (Sorokin and Yaschenko, 1999), but also the presence of powerful lithospheric source of the electric field is necessary for this.

References

Didebulidze, G.G., Fishkova, N.M., Pataraya, A.D., Toroshelidze, T.I., 1990. Investigation of the night sky airglow near the epicenter of the earthquake. In: Proceedings of the Joint Varenna-Abastumani-ESA-Nagoya-Potsdam Workshop on "Plasma Astrophysics", Telavi, Georgia, USSR, 4–12 June (ESA SP-311, August 1990), pp. 321–327.

Dzubenko, M.I., Ivchenko, V.M., Kozak, L.V., 2001. Temperature variations over earthquake epicenters from observations obtained by the UARS satellite. Space Sci. Technol. (Kosmichna nauka i tehnologiya, Ukraine) 7, 94–99.

Dzubenko, M.I., Ivchenko, V.M., Kozak, L.V., 2003. Temperature variations in the thermosphere over the earthquake focuses as inferred from satellite data. Geomagn. Aeronomy 43, 118–123.

Fuks, I.M., Shubova, R.S., Martynenko, S.I., 1997. Lower ionosphere response to conductivity variations of the near-earth atmosphere. J. Atmos. Terr. Phys. 59, 961–965.

Gladishev, V.A., Fishkova, L.M., 1994. Optical research of seismoactivity effects of the ionosphere. In: Hayakawa, M., Fujinawa, Y. (Eds.), Electromagnetic Phenomena Related to Earthquake Prediction. Terrapub, Tokyo, pp. 375–380.

Gokhberg, M.B., Nekrasov, A.K., Shalimov, S.L., 1996. To the influence of nonstable release of green-effect gases in seismically active regions on the ionosphere. Phys. Earth (Fizika Zemli) 8, 52–55 (in Russian).

Gotynyan, O.E., Ivchenko, V.M., Rapoport, Yu.G., 2001. Model of the internal gravity waves excited by lithospheric greenhouse effect

gases. Space Sci. Technol. (Kosmichna nauka i tehnologiya) 7 (2), 26–33.

Gotynyan, O.E., Ivchenko, V.M., Rapoport, Yu.G., Parrot, M., 2003. Ionospheric disturbances excited by the lithospheric gas source of acoustic gravity waves before earthquakes. Space Sci. Technol. (Kosmichna nauka i tehnologiya, Ukraine) 9 (2), 89–105.

Grimalsky, V.V., Kremenetsky, I.A., Rapoport, Y.G., 1999. Excitation of electromagnetic waves in the lithosphere and their penetration into ionosphere and magnetosphere. J. Atmos. Electr. 19 (2), 101–117.

Grimalsky, V.V., Kremenetsky, I., Cheremnykh, O.K., Rapoport, Yu.G., 2002. Spatial and frequency filtration properties of ULF EM radiation of lithospheric origin in the lithosphere–ionosphere–magnetosphere system. In: Hayakawa, M., Molchanov, O.A. (Eds.), Seismo Electromagnetics: Lithosphere–Atmosphere–Ionosphere Coupling. TERRUPUB, Tokyo, pp. 363–370.

Grimalsky, V.V., Hayakawa, M., Ivchenko, V.N., Rapoport, Yu.G., Zadoroznii, V.I., 2003. Penetration of an electrostatic field from the lithosphere into the ionosphere and its effect on the D-region before earthquakes. J. Atmos. Solar-Terr. Phys. 65, 391–407.

Gurevich, A.V., 1978. Nonlinear Phenomena in the Ionosphere. Springer-Verlag Publ. House, New York.

Hayakawa, M., Molchanov, O.A., Ondoh, T., Kawai, E., 1996. The precursory effect of the Kobe earthquake on VLF subionospheric signals. J. Comm. Res. Lab. 43, 169–180.

Huixin, S., Zuhuang, C., 1986. Geochemical characteristics of underground fluids in some active fault zones in China. J. Geophys. Res. 91 (B12), 12,282–12,290.

Martinenko, S.I., 1989. On the modeling of electron concentration perturbations in the D region of the ionosphere caused by energetic particle flows. Geomagn. Aeronomy 29, 64–70.

Molchanov, O.A., Hayakawa, M., 1994. Generation of ULF seismogenic electromagnetic emission: a natural consequence of microfracturing. In: Hayakawa, M., Fujinawa, Y. (Eds.), Electromagnetic Phenomena Related to Earthquake Prediction. TERRUPUB, Tokyo, pp. 537–563.

Molchanov, O.A., Hayakawa, M., 1998. Subionospheric VLF signal perturbations possibly related to earthquakes. J. Geophys. Res. 103 (A8), 17489–17504.

Molchanov, O.A., Hayakawa, M., Miyaki, K., 2001. VLF/LF sounding of the lower ionosphere to study the role of atmospheric oscillations in the lithosphere–ionosphere coupling. Adv. Polar Upper Atmos. Res. 15, 146–158.

Molchanov, O.A., Hayakawa, M., Rafalsky, V.A., 1995. Penetration characteristics of electromagnetic emission from an underground seismic source into the atmosphere, the ionosphere, and magnetosphere. J. Geophys. Res. 100A, 1691–1712.

Molchanov, O.A., Hayakawa, M., Afonin, V.V., Akentieva, O.A., Mareev, E.A., Trakhtengerts, V.Yu., 2002. Possible influence of siesmicity by gravity waves on the ionospheric equatorial anomaly from data of IK-24 satellite. 2. Equatorial anomaly and small-scale ionospheric turbulence. In: Hayakawa, M., Molchanov, O.A. (Eds.), Seismo Electromagnetics: Lithosphere–Atmosphere–Ionosphere Coupling. TERRUPUB, Tokyo, pp. 287–296.

Ogawa, T., Shimazaki, T., 1975. Diurnal variations of odd nitrogen densities in the mesosphere and lower thermosphere: simultaneous solution on photochemical-diffusive equations. J. Geophys. Res. 80, 3945–3960.

Ossakov, S., 1981. Spread-F theories—a review. J. Atmos. Terr. Phys. 43, 437.

Oster, A., 1965. Remarks on the problem of radioactive accumulation of ground's surface. In: Coroniti, S.C. (Ed.), Problems of Atmospheric Electricity, Proceedings of the Third International Conference on Atmosphere and Space Electricity, Montreux, Switzerland, 5–10 May 1963. Elsevier Publ. Co, Amsterdam, pp. 121–122.

Rowe, J.N., Mitra, A.P., Ferraro, A.J., Lee, H.S., 1974. An experimental and theoretical study of the D-region—II. A semi-empirical model for mid-latitude D-region. J. Atmos. Terr. Phys. 36, 755–785.

Sorokin, V.M., Yaschenko, A.K., 1999. Disturbance of conductivity and electric field in the Layer Earth–Ionosphere above the earthquake preparation region. Geomagn. Aeronomy 39, 100–106.

Tohmatsu, T., Ogawa, T., 1991. Compendium of Aeronomy. TERRUPUB, Tokyo.

Tomko, A.A., Ferraro, A.J., Lee, H.S., Mitra, A.P., 1980. A theoretical model of D-region ion chemistry modifications during high power radio wave heating. J. Atmos. Terr. Phys. 42, 275–285.

Vershinin, E.F., Buzevich, A.V., Yumoto, K., Saita, K., Tanaka, Y., 1999. Correlation of seismic activity with electromagnetic emissions and variations in Kamchatka region. In: Hayakawa, M. (Ed.), Atmospheric and Ionospheric Electromagnetic Phenomena Associated with Earthquakes. Terrapub, Tokyo, pp. 513–517.